

# Design of a Bipedal Walker with a Passive Knee and Parted Foot

Honggu Lee and Sungho Jo

Dept. of Computer Science, KAIST  
291 Daehak-ro, Yuseong-gu, Daejeon 305-701, Korea  
{nickplay, diskedit, shjo}@kaist.ac.kr

**Abstract.** The design of a bipedal walker that enables a human-like, compliant walking motions with simple control commands is presented. The design includes a passive knee bending/stretching mechanism with a latch hinge and a parted foot structure with compliant spring-based actuation. In addition, the leg posture, asymmetric lateral spring placement, round ankles, active hip sway, pelvic tilt actuation, and provisions for simple control were designed to implement the desired walking motion. The prototype bipedal walker was built with a combination of passive and actuated joints, utilizing springs around the joints for further compliancy. Experiments were conducted using the prototype bipedal walker in order to evaluate the design.

**Keywords:** Bipedal walker, compliant, passive knee, parted foot.

## 1 Introduction

The design of a bipedal robot which walks with human-like motion, has been a daunting yet exciting research topic. It is very challenging to realize natural, human-like robot walking motions due to how the knee bends and the contact made by the foot on the ground. A common approach to bipedal motion is to tightly control the joint angles so that they mimic human walking motions. Honda Asimo and KAIST Hubo are two famous prototype robots that have been created in order to conduct research on dynamic locomotion [1, 2]. However, these designs have used knee bending while walking to maintain stability [1-4]. The Hubo laboratory recently manufactured a stretched-leg walking robot. However, this robot has a flat foot and ankle-level push off is not used often because maintaining stability is difficult [5]. Another robot, Humanoid H6, has toe joints [6] which increases its walking speed, and the joints enable climbing steps. Even though these impressive technological advances in robotics have been realized, further investigation is required in order to create more natural walking motions.

Another approach to natural-gait robot motions is based on passive-dynamic walkers. These walkers have minimal or no actuators and a simple control strategy [7-10]. It is known that this approach is advantageous for efficient energy consumption and gait appearance. The Cornell Powered Biped is based on the

passive-dynamic walker model, and it has a passive knee mechanism that realizes knee bending and stretching while avoiding hyperextension. In order to bend the knees, the passive-dynamic walker requires a controllable solenoid. Furthermore, the feet must be rounded in order to walk smoothly [9, 10]. However, the passive-dynamic walking strategy may hinder implementing precise or adaptive behaviors. Therefore, a robot design that incorporates the advantages of both approaches is a natural progression for the next generation of technologies for bipedal robot locomotion [11, 12].

This study investigates a design that may be effective in generating human-like walking motions in a robot using a small number of actuators. As a preliminary step, this work designs and manufactures a prototype bipedal walking robot based on insights attained from studying human gaits.

The prototype design adopts two visual aspects of the human gait. The first is a bending and stretching knee motion. McGeer noted the practical advantages of the knee motion for walking legs [7]; the knee bending prevents feet from colliding with the ground during the leg swing and the knee absorbs any impact while the foot is contacting the ground for stability. This proposed knee mechanism is implemented passively without actuators. The second aspect of human motion that is adopted is the motion by which the foot comes into contact with the ground. The human foot is flexible when engaging in toe-off and heel-strike motions [13]. Thus, the foot design was carefully planned in order to achieve compliancy when interacting with the ground. In order to mimic the toe-off and heel-strike motions, a two-part foot design was used.

## 2 Mechanical Design

The prototype is 46.7 cm tall and weighs 1.7 kg. It consists of two legs, two feet, and a small torso. Within each leg, the thigh and shank are 13.8 cm and 14.3 cm long, respectively. Each leg has 5 degrees of freedom (DOFs): two at the hip, one at the knee, and two at the ankle. In a three-dimensional space, each leg is actuated by three servomotors (Dynamixel RX-28, Robotis, Inc. [14]), which are labeled M1, M2, and M3 in Fig. 1. M1 and M2 realize the lateral and forward-backward swing of a leg from the hip, respectively. M3 enables the ankle flexion and extension. In each leg, three passive joints, indicated by P1, P2, and P3 in Fig. 1, are included. P1 is a lateral hip joint, P2 indicates the knee joint, and P3 is the lateral ankle joint.

### 2.1 Foot and Toe Design

Each foot consists of two parts: a forefoot(toes) and a rearfoot(heel) (Fig. 2(a)). The fore and rear sections are 40 and 70 mm long, respectively. The forefoot is connected to the rear-foot via joints while being supported by a pair of passive springs (labeled as S1 in Fig. 2; only one side shown). The split foot design aims to improve the robot maneuverability during the push-off or ground-touch motions. One end of S1 is attached to a roller located on the forefoot so that it can be pulled when the forefoot touches the ground and the rearfoot is off the ground. The pulling stores the elastic

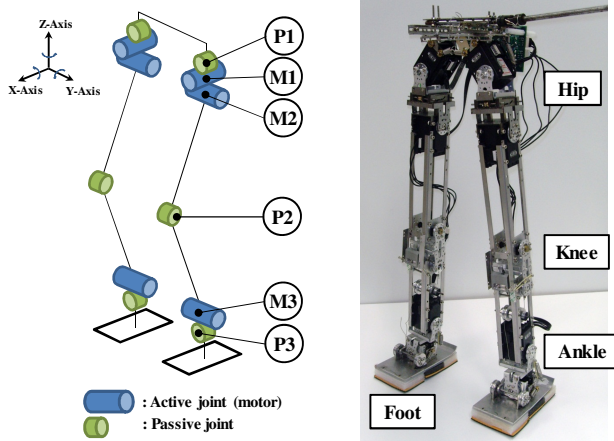


**Fig. 1.** (a) Kinematic details of (b) the proposed bipedal walker

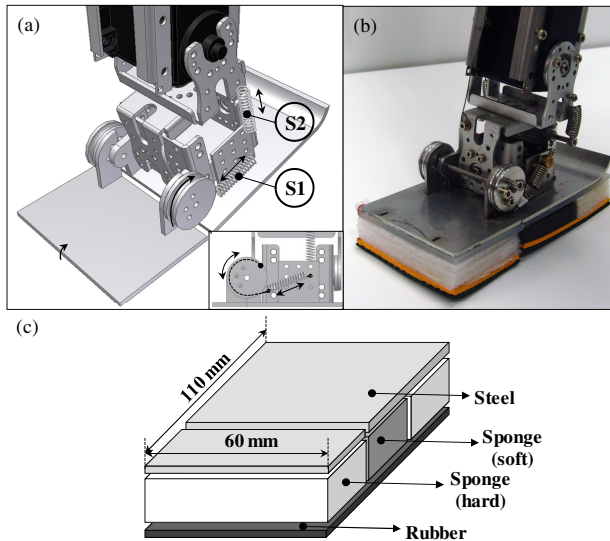


**Fig. 2.** (a) Parted foot design, (b) assembled foot, and (c) layered foot structure

energy in S1. During the ankle push-off motion, the forefoot pushes the ground by releasing the elastic energy. The push-off thrusts the upper robot body forward.

Passive-dynamics-based walking robots use similar strategies in order to minimize the motor power requirements for the push-off motion [7-10]. These robots usually have push-off springs at the ankle joint in order to achieve the ankle extension. However, in the proposed robot, the push-off springs are operated via the joint between the toe and the foot body.

This design was chosen for the following reasons. Generally, other bipedal robots have solid feet, so the ankle joint must rotate the feet. With solid feet, the ankle

extension in the standing leg requires a large amount of potential energy within the spring in order to lift the upper body, but it produces a large forward thrust once the foot is off the ground, increasing the difficulty in maintaining the gait stability. In order to moderate this issue, robots usually have curved bottoms of their feet. However, these robots can still produce high forward thrust and thus require careful control in order to achieve stable leg swing motions during the swing phase and stable ground touches at the swing-to-stand transition. For example, the push-off process is mechanically constrained just after the heel strike in reference [7].

In the proposed robot, an appropriate amount of potential energy in the spring is required for the joint extension between the forefeet and rearfoot, which is designed to perform the push-off. Therefore, in this study, a flat but two-parted foot in the prototype enables compliant stable motions.

During the foot landing, the rearfoot touches the ground before the forefoot. The whole foot bottom is layered with the sponge and rubber materials that are used in table tennis racquets. These materials provide a damping effect similar to the skin and flesh of a foot. In particular, the toes and heels have hard sponges to provide sufficient pushing force during push-off and to achieve sufficient impact absorption on landing. In the proposed robot, while the spring pair S1 pushes against the ground, the active motors at the hip and in the standing leg user power to move the whole body forward. Therefore, the proposed robot has both the passive and active dynamic characteristics of walking. A pair of passive springs (labeled S2 in Figure 2) between the heel and shank is also influential during landing. The S2 pair assists in maintaining lateral balance. Furthermore, while the opposite leg kicks the ground, the S2 pair alleviates its impact on the ankle of the standing leg. Thus all of the passive springs around the foot and ankle yield compliant motions.

## 2.2 Ankle Design

The shank and foot are connected via an ankle joint with the M3 motor, as shown in Fig. 3. The motor body is rigidly attached to the end of the shank, and its shaft rotates the foot in a sagittal plane. From the heel-strike to the toe-off, the motor assists the upper body to move around the ankle joint of the standing leg in the same manner as

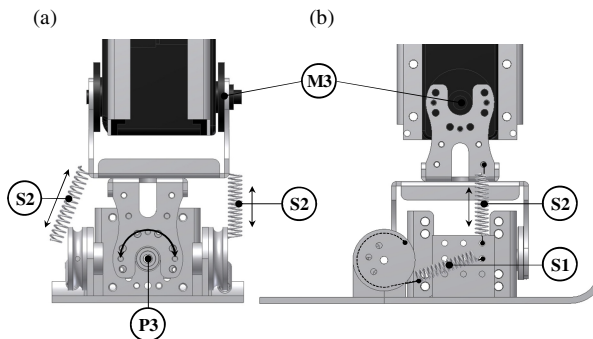


**Fig. 3.** The (a) front and (b) side view of the compliant ankle mechanism

an inverted pendulum would. The ankle rotation using M3 critically affects the push-off motion because the push-off thrust is most effective when the foot rotation and body orientation are properly synchronized. Furthermore, M3 can control the relative posture of the foot to the body orientation. Therefore, the motor motion is important for gait efficiency and stability.

As mentioned in the previous section, the spring pair S2, located on each side of the ankle, generates the compliant rotational motion in the coronal plane around the passive joint P3. The S2 pair support the shank laterally and damp the contact impact in the coronal plane. The structure was designed so the outer S2 is tensed relative to the inner S2 when the foot is on the ground, as shown in Fig. 3(a). This design supports the standing leg while the other leg swings, and it maintains the robot's posture at the heel-strike.

The space between the legs is slightly wider at the foot than at the hip. This posture helps generate the lateral directional motion and aids lateral balancing. In addition, the foot is designed to tilt slightly inward through the use of a stiffer spring inside than that used outside. During push-off, the leg posture and asymmetric spring strength help pull the standing leg to protect the lateral stability from outward sway. Each spring's stiffness is tuned empirically. The ankle motion in the sagittal plane also influences the knee bending and extending mechanism, which is discussed in the next section.

### 2.3 Knee Design

The knee mechanism is designed to prevent hyperextension and to bend or extend the lower leg at the passive joint P2. The knee joint is locked after the mid-swing until the end of the standing phase and is unlocked during the remainder phase. As shown in Figures 4(a) and 4(b), the locking mechanism is essentially a type of latch. The full cycle of the knee bending and extending procedure is illustrated in Figure 4(c). A latch arm is attached to the shank using a hinge with a torsion spring and the latch body is rigidly attached to the thigh (see Figures 4(d) and 4(e)). A torsion spring pushes the latch arm to maintain a lock during extension.

At the ankle push-off, the ankle angle (M3) reaches a threshold value ( $10^\circ$ , as shown in Figure 4(c)); then, the latch arm is pulled by a string connected via three pulleys to the foot. The string pull is sufficiently strong to overcome the torsion spring. Therefore the latch arm is detached from the latch body as seen in Figure 4(d). The string is minimally strained even without the ankle's substantial pulling force and does not disconnect from the pulleys. The pulleys translate the linear pulling force generated from the foot rotation (at the ankle push-off) to the latch arm. This detachment allows the knee to start bending. After unlocking, the knee flexes using the motion inertia. The tip of the latch body is connected to the top of the shank by a rubber band. While the knee bends, the rubber band gains elastic energy, which is used to change the inertia of the shank after sufficient bending. Next, the motion's inertia drives the shank back to stretch the leg during the forward swing phase.

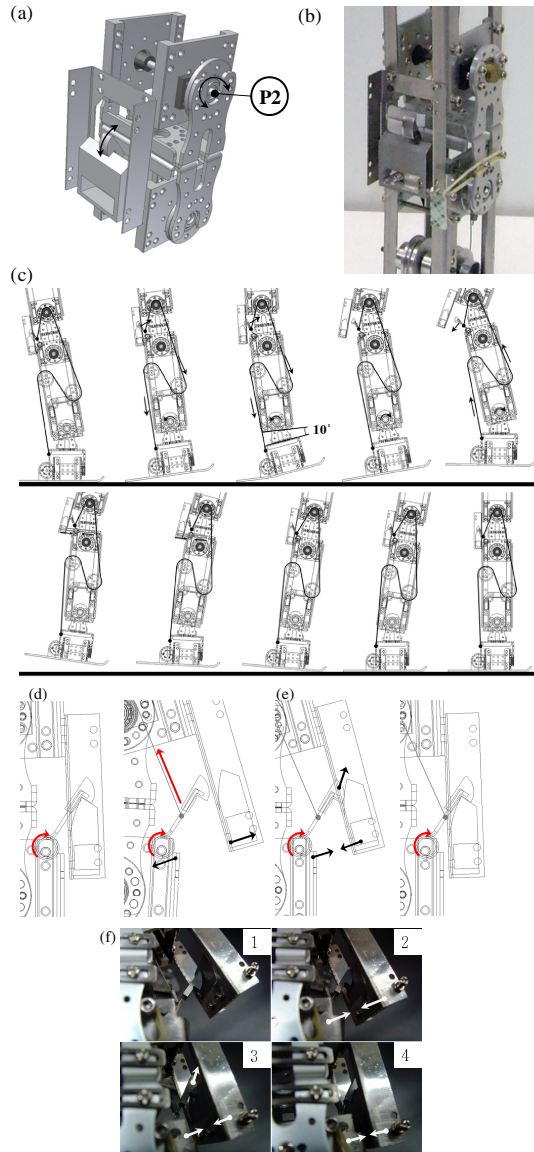


**Fig. 4.** (a) Passive knee design and (b) its implementation. (c) Knee bending and extending mechanism over a gait cycle (d) knee release, and (e) & (f) knee locking.

While extending the shank via the knee joint, the ankle’s angle remains less than the threshold value, and the string does not pull on the latch arm. The torsion spring clips the hook on top of the latch arm into the slit of the latch surface to engage the locking, as shown in Figure 4(e). The leg is then extended. Both the hook and latch surfaces have curvature. The hook moves along the latch surface with a line contact to

minimize friction. Figure 4(f) illustrates the overall knee locking procedure. The knee mechanism is passive and does not require electric power for operation.

## 2.4 Hip and Pelvis Design

The pelvis and both legs are joined at the hip. A drive motor is located on each hip. A motor, indicated as M2 in Fig. 5, is attached to the thigh drive's forward-backward swing relative to the pelvis. Another motor (M1) enables the leg to be moved laterally. The M1 actuation enables adequate lift of the swing leg for swing clearance, mimicking the pelvic tilt of human gait [13]. When M1 lifts the pelvis, the rotation at joint P1 is blocked by a clamp (Figure 5(b)), thus allowing the swing leg to be lifted. When M1 releases the pelvis, spring S3 holds the leg laterally. The spring aids lateral balancing during ground contact. The motors used in this robot are controlled by a compatible controller board (CM-2+, Robotics, Inc.) attached to the pelvis frame (see Fig. 1.)

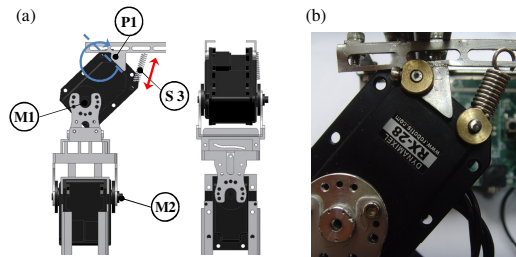


Fig. 5. (a) Hip and pelvis design and (b) its implementation

## 2.5 Parameter Fine-Tuning

In order to implement the proposed mechanism, some parameter values must be determined such as the spring values. All passive spring coefficients were selected via trial and error. The robot was tested progressively with physical tinkering, because analysis of the numerous effects of a bipedal walker with passive parts is difficult to simulate and characterize. Thus, analytic modeling was not undertaken for this robot. The selected springs S1 and S3 have the same stiffness, and S2 has less stiffness.

## 3 Control Command Profiles

The command profiles were adopted from typical human gait joint profiles in order to generate human-like motion [13]. The profiles were modified empirically to enable the proposed robot to implement reasonable walking motions through trial and error. In order to implement walking, the input trajectories were sent to the motors from a PC through the controller. Figure 6 shows the commands, which indicate the desired active joints' angular trajectories. The command trajectory for M1 was designed to

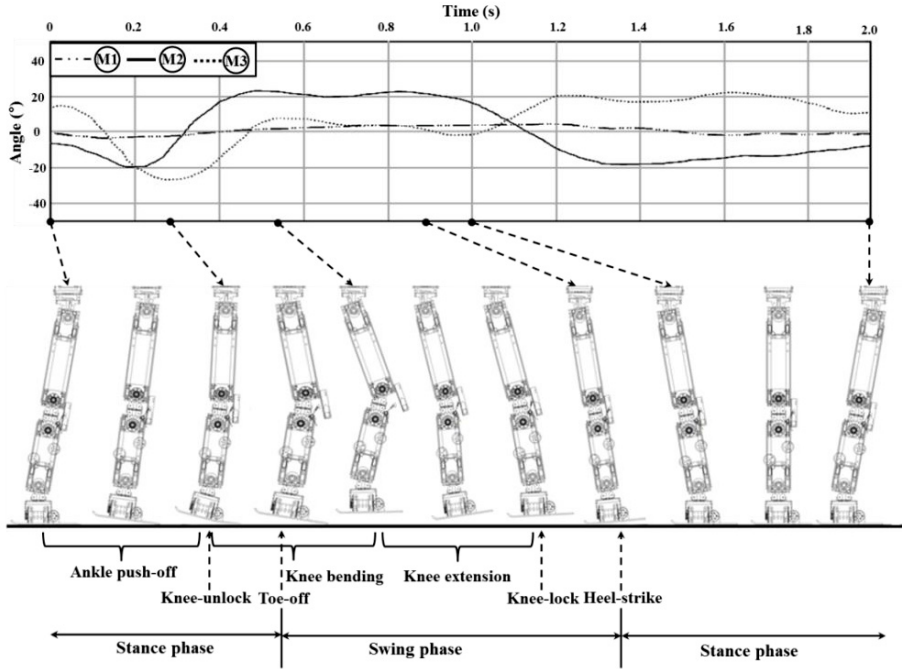


Fig. 6. Control command profiles and desired robot motion during a gait cycle

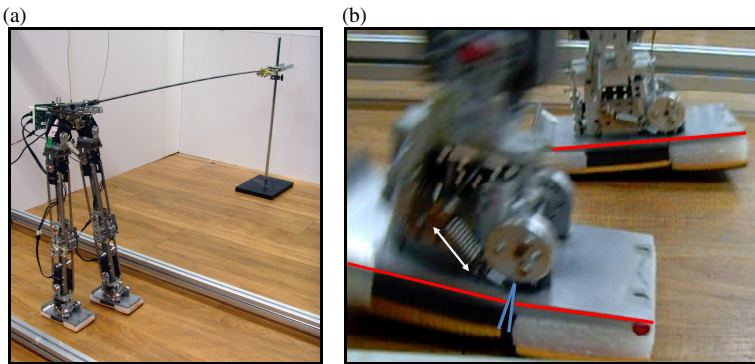


Fig. 7. (a) Experimental setup, (b) Snapshot of the two-part feet at push-off

activate a slight lateral sway at the hip, while the command trajectory for M2 activates the forward-backward swing of the leg at the hip. The command trajectory for M3 describes the ankle motion. In the early phase of the plot, the ankle flexion stretches the S1 spring pair in order to obtain elastic energy. The command profile is a feed-forward profile: the gait cycle is designed to last 2 seconds in the current stage. Different phases and gait events are shown in figure 6 as well.

## 4 Experimental Results

Figure 7 (a) shows the experimental setup for the proto-type walking robot. The robot was mounted on a boom, which provided lateral stability while still permitting nontrivial lateral motion. Table 1 summarizes the specifications of the prototype robot walker.

**Table 1.** The Specifications of the bipedal walker

Weight (kg)	1.7		D.O.F	Hip	6
Dimesions (mm)	Height	467		Knee	2
	Width	175		Ankle	4
	Depth	120		Total	12

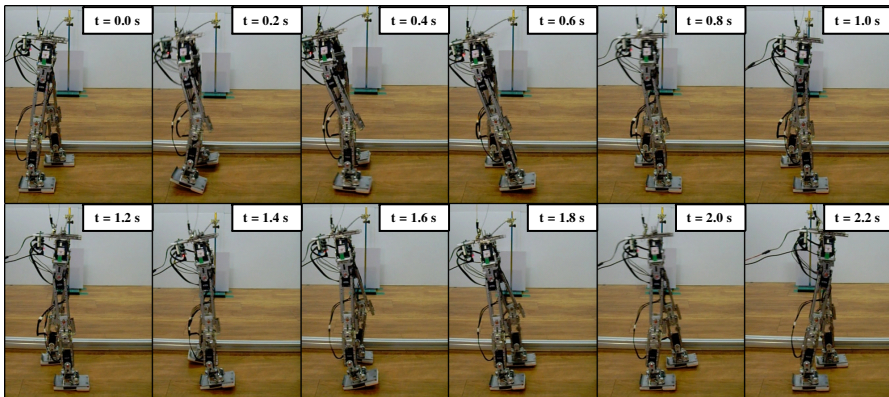
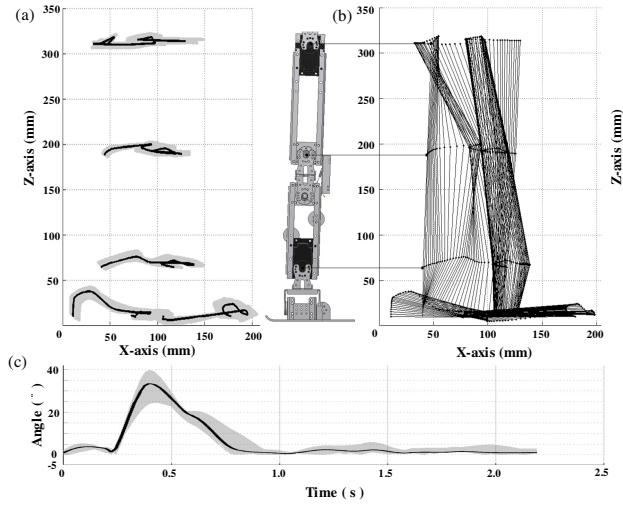


**Fig. 8.** Sequential snapshots of walking performance

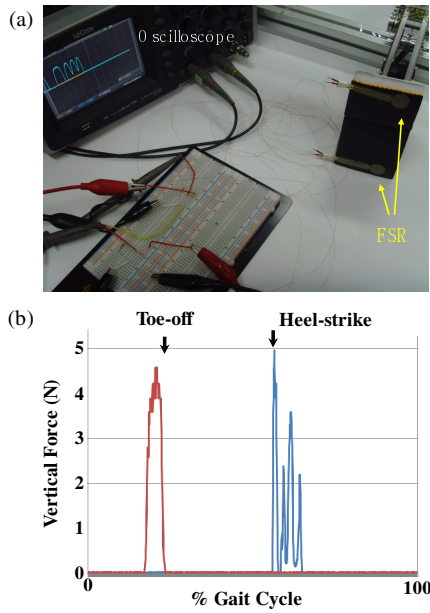
Figure 8 shows sequential snapshots of the robot's walk taken during the experiment. Figure 7(b) demonstrates the instant of the S1 spring's pulling motion during push-off. The forefoot and rearfoot parts are misaligned.

Figure 9 analyzes the detailed joint motions. In Figure 9(a), each joint trajectory is described as Cartesian coordinate points and Figure 9(b) draws the corresponding stick plots. Figure 9(c) shows the knee joint trajectory in degrees over time. The bending and stretching motions are clearly seen. The thick line represents the averaged profile over five trials, and the grayed region indicates the standard deviations. Figure 9 verifies that the passive knee mechanism works as expected.

While the prototype walked, the reaction force on the bottom of the foot was measured using the system shown in Figure 10(a). Each force sensor (Standard 402 Force Sensing Resistors (FSR), Interlink Electronics, Inc. [15]) was attached on the forefoot and rearfoot sections. The sensor measured the point contact force. The measured contact force is shown in Figure 10(b). The peak vertical reaction force at



**Fig. 9.** (a) Joint motions, (b) stick plots, and (c) measured knee joint angle trajectories while the prototype robot was walking



**Fig. 10.** Reaction force measuring: (a) setup and (b) profiles

the forefoot occurred during ankle push-off while the peak vertical force of the rearfoot occurred during the ground contact. The two peak profiles are separate, which indicates that one foot part is off the ground in each phase, and the peak magnitudes are approximately equal. This observation indicates that the different parts of the foot operated in a similar manner as human feet [13]. The sensors measured the vertical reaction forces at a spot on each forefoot and rearfoot; therefore, the measurements do not indicate the total reaction forces over the entire foot. The parted foot and ankle structures surrounded by springs provided a compliant gait motion.

## 5 Conclusion

This study presented the design of a bipedal walker that focuses on the mechanical design for human-like gait motions. The robot design is a proof of concept prototype that may provide insights into the design of bipedal walkers with respect to a passive knee and parted foot design. The experimental observations verified that the design is amenable to a compliant walking motion. The prototype enables knee bending, toe-off, and heel-strike motions which are similar to the human gait. Furthermore knee bending and stretching during the gait was achieved. The spring-based actuation at ankle push-off provided partial forward thrust, and the active hip and ankle actuations moved the robot body forward. The pelvic tilt actuation provided clearance for the swinging leg.

For more complicated walking tasks, the proposed mechanism must be further developed. The passive knee and parted foot mechanism ensure stability on a flat surface but not in other environments. An interesting topic for future development would be the design of a simple mechanism that can modify the knee bending angles adaptively even though they are passive. In addition, the current algorithm is a feed-forward algorithm, and the robot's performance is sensitive to its initial conditions. Furthermore, robust balance control was not seriously considered. An advanced control mechanism could provide a variety of robust gait.

## References

1. Hirai, K., Hirose, M., Haikawa, Y., Takenaka, T.: The Development of Honda Humanoid. In: IEEE International Conference on Robotics and Automation, vol. 2, pp. 1321–1326 (1998)
2. Park, I., Kim, J., Lee, J., Oh, J.: Mechanical Design of Humanoid Robot Platform KHR-3 (KAIST Humanoid Robot-3: Hubo). In: IEEE-RAS International Conference on Humanoid Robots, pp. 321–326 (2005)
3. Gouaillier, D., Hugel, V., Blazevic, P., Kilner, C., Chris, M.: Mechatronic Design of NAO Humanoid. In: IEEE International Conference on Robotics and Automation, pp. 769–774 (2009)
4. Kaneko, K., Harada, K., Kanehiro, F., Miyamori, G., Akachi, K.: Humanoid Robot HRP-3. In: IEEE/RSJ International Conference on Intelligent Robots and Systems, pp. 2471–2478 (2008)

5. Kim, M., Kim, I., Park, S., Oh, J.: Realization of stretch-legged walking of the humanoid robot. In: IEEE-RAS International Conference on Humanoid Robots, pp. 118–124 (2008)
6. Nishiwaki, K., Kagami, S., Kuniyoshi, Y., Inaba, M., Inoue, H.: Toe joints that enhance bipedal and fullbody motion of humanoid robots. In: IEEE International Conference on Robotics and Automation, vol. 3, pp. 3105–3110 (2002)
7. McGeer, T.: Passive Dynamic Walking. *International Journal of Robotics Research* 9, 62–82 (1990)
8. Garcia, M., Chatterjee, A., Ruina, A.: Efficiency, speed, and scaling of two-dimensional passive-dynamic walking. *Dynamics and Stability of Systems* 15, 75–99 (2000)
9. Collins, S., Ruina, A.: A Bipedal Walking Robot with Efficient and Human-Like Gait. In: IEEE International Conference on Robotics and Automation, pp. 1983–1988 (2005)
10. Collins, S., Ruina, A., Tedrake, R., Wisse, M.: Efficient Bipedal Robots based on Passive-dynamic Walkers. *Science* 307, 1082–1085 (2005)
11. Kuo, A.: Energetics of Actively Powered Locomotion using the Simplest Walking Model. *Transactions-American Society of Mechanical Engineers, Journal of Biomechanical Engineering* 124, 113–120 (2002)
12. Wu, T., Yeh, T.: Optimal Design and Implementation of an Energy-efficient Biped Walking in Semi-active Manner. *Robotica* 27, 841–852 (2008)
13. Perry, J.: Gait Analysis: Normal and Pathological Function. *Journal of Pediatric Orthopaedics* 12, 815 (1992)
14. Robotis©, Dynamixel, [http://www.robotis.com/xen/dynamixel\\_en](http://www.robotis.com/xen/dynamixel_en)
15. Interlink Electronics©. FSR 400 Series, <http://www.interlinkelectronics.com/Product/Standard-402-FSR>